研　究　速　報

UDC 517.544 : 518.61

NUMERICAL EXPERIMENTS OF HIGHER-ORDER APPROXIMATE SOLUTIONS OF NEUMANN PROBLEMS

ノイマン問題に対する高精度近似解の数値実験

by Masahisa TABATA*

田 端 正 久

1. Introduction

Recently the author has considered a higher-order approximate procedure for the Neumann problem using the isoparametric finite element method with the relevant lumping operator and he has obtained the optimal order of convergence [1]. The present paper is a report of the numerical experiments on such a problem. For Poisson's equation with inhomogeneous Neumann boundary condition in a domain with a curved boundary, several finite-element procedures are constructed by using piecewise linear or piecewise quadratic basis functions and some relevant lumping operators. For each procedure a series of approximate solutions are obtained by subdividing the domain and its convergence order is compared with the theoretical one.

2. Notations and Theoretical Reuslts

Let Ω denote a bounded domain in R^2 with boundary Γ, which is sufficiently smooth. Let $H^m(\Omega)$ be the usual Sobolev space and its norm is given by

$$\|u\|_{m,\Omega}=\left\{\sum_{|\alpha|\le m}\int_\Omega |D^\alpha u|^2\,dxdy\right\}^{1/2},$$

where $\alpha=(\alpha_1,\alpha_2)$, α_1 and α_2 are non-negative integers,

$$|\alpha|=\alpha_1+\alpha_2 \quad\text{and}\quad D^\alpha u=\frac{\partial^{|\alpha|}u}{\partial x^{\alpha_1}\partial y^{\alpha_2}}$$

$H^0(\Omega)$ is usually expressed as $L^2(\Omega)$. Throughout the present paper the following notations are used,

$$(f,v)=\int_\Omega f\cdot v\,dxdy \quad \text{for } f,v\in L^2(\Omega), \tag{1}$$

$$a(u,v)=(\partial u/\partial x,\ \partial v/\partial x)+(\partial u/\partial y,\ \partial v/\partial y) \quad \text{for } u,v\in H^1(\Omega), \tag{2}$$

and

$$[g,\ v]=\int_\Gamma g\cdot v\,dt \quad \text{for } g,v\in L^2(\Gamma). \tag{3}$$

We consider the following problem,

$$\begin{cases} -\Delta u=f & \text{in } \Omega \\ du/dn=g & \text{on } \Gamma. \end{cases} \tag{4}$$

Here $\Delta=\partial^2/\partial x^2+\partial^2/\partial y^2$ and n refers to the outer normal to Γ. In order that a solution exists it is necessary that the inhomogeneous data, f and g, satisfy the condition

$$(f,\ 1)+[g,\ 1]=0. \tag{5}$$

If f and g have appropriate smoothness, a solution exists in $H^m(\Omega)$ uniquely under the condition

$$(u,\ 1)=0, \tag{6}$$

for some m.

We triangulate Ω so that all the angles of the triangles are greater than some positive number. Let T_0 be a closed fundamental triangle with vertices $A_1(0,\ 1)$, $A_2(0,\ 0)$ and $A_3(1,\ 0)$. In T_0 there exist k fundamental nodal points, $\{A_i\}_{i=1}^k$, including three vertices. Let $\Psi=\{\hat\phi_i\}_{i=1}^k$ be the set of the fundamental basis functions corresponding to $\{A_i\}_{i=1}^k$ such that

$$\hat\phi_i(A_j)=\delta_{ij} \quad \text{for } i,\ j=1,\ldots,k,$$

and $\hat\phi_i=0$ on any side which does not contain A_i, $i=1,\ldots,k$. Required points are added in $\bar\Omega$ so that there exist k nodal points in the neighbourhood of each triangle. (Three of them are vertices of its triangle, and most of them are shared with the neighbouring triangles.) Let N be the total number of all the nodal points in $\bar\Omega$ and $\{P_i\}_{i=1}^N$ be the set of the numbered nodal points. Let $\{B_i^j\}_{i=1}^k$ be the set of nodal points for the j-th triangle. (B_1^j, B_2^j and B_3^j are vertices.) Then $F_j=\sum_{i=1}^k B_i^j\hat\phi_i\in\Psi\hat{\times}\Psi$, which satisfies

$$F_j(A_i)=B_i^j \quad \text{for } i=1,\ldots,k,$$

determines an isoparametric finite element K_j as

$$K_j=F_j(T_0).$$

Let Ω_h be the interior of the union of all the iso-

* Dept. of Mechanical Engineering and Naval Architecture, Inst. of Industrial Science, Univ. of Tokyo.

parametric finite elements and Γ_h be its boundary. We define the trial function space $S(\Omega_h)$, as a N dimensional subspace of $H^1(\Omega_h)$ spanned by $\{\hat{\phi}_i\}_{i=1}^N$. Here

$$\hat{\phi}_i = \sum_{i=1}^{K} \delta(P_i, B_i^j)\bar{\phi}_i(F_j^{-1}) \text{ in each } K_j,$$

where $\delta(P_i, B_i^j) = 1$ if $P_i = B_i^j$ and $=0$ otherwise. Let P be an interpolating operator from $C(\Omega_h)$ into $S(\Omega_h)$ such that

$$Pu = \sum_{i=1}^{N} u(P_i)\hat{\phi}_i,$$

where $C(\bar{\Omega}_h)$ consists of all the continuous functions in $\bar{\Omega}_h$. We consider $\{\bar{\psi}_i\}_{i=1}^k$ in T_0, which is associative with $\{\bar{\phi}_i\}_{i=1}^k$. (Some conditions are imposed on $\{\bar{\psi}_i\}_{i=1}^k$. See [1].) Then Q, a lumping operator from $C(\bar{\Omega}_h)$ into $L^2(\Omega_h)$, is defined similarly to P replacing $\hat{\phi}_i$ by $\bar{\phi}_i$.

The finite element solution of (4) and (6), which we consider, is $\hat{u} \in S(\Omega_h)$ such that

$$a_h(\hat{u}, \hat{\phi}) = (f_1, Q\hat{\phi})_h + [g_A, \hat{\phi}]_h \text{ for any } \hat{\phi} \in S(\Omega_h), \quad (7)$$

and

$$(\hat{u}, 1)_h = 0, \quad (8)$$

where $f_1 = Pf - k_2$, $g_A = Pg$, $k_2 = \{(Pf, 1)_h + [Pg, 1]_h\}/\text{mes}(\Omega_h)$, and $(f, v)_h$, $a_h(u, v)$ and $[g, v]_h$ are defined by replacing Ω and Γ with Ω_h and Γ_h in (1), (2) and (3).

Remark 1 : It should be noted that Pg on Γ_h is determined only by the nodal values of g on Γ. (See the definition of Ψ.)

Remark 2 : (7) forms N linear equations, but they are linearly dependent in virtue of k_2.

Now let us consider some concrete examples of P and Q which are used in numerical experiments.

Example 1.

k= 3 and $\{\bar{\psi}_i\}_{i=1}^3$ is as follows :

$$\bar{\psi}_1 = \eta,$$

$$\bar{\psi}_2 = 1 - \xi - \eta,$$

and

$$\bar{\psi}_3 = \xi.$$

This is the usual piecewise linear basis. Then three kinds of Q are considered. In the first case $\{\bar{\psi}_i\}_{i=1}^3$ is as follows:

$\bar{\psi}_1 = 1$ in S_1 and $= 0$ otherwise,

$\bar{\psi}_2 = 1$ in S_2 and $= 0$ otherwise,

and

$\bar{\psi}_3 = 1$ in S_3 and $= 0$ otherwise,

where S_1 is a quadrilateral with vertices A_1, A_4, G and A_6, and S_2 and S_3 are taken similarly. (See Fig. 1.)

In the second case,

$$\bar{\psi}_1 = \bar{\psi}_2 = \bar{\psi}_3 = 1/3.$$

In the third case,

$$\bar{\psi}_i = \hat{\psi}_i \quad \text{for } i = 1, 2, 3.$$

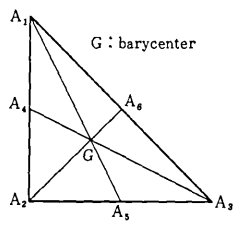

Fig. 1 Fundamental triangle

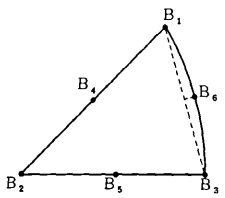

Fig. 2 Curved element

Example 2.

k=6. We take A_4, A_5 and A_6 at the midpoints of A_1A_2, A_2A_3 and A_3A_1 respectively. $\{\bar{\psi}_i\}_{i=1}^6$ is as follows :

$$\bar{\psi}_1 = \eta(2\eta - 1),$$

$$\bar{\psi}_2 = (1 - \xi - \eta)\{1 - 2(\xi + \eta)\},$$

$$\bar{\psi}_3 = \xi(2\xi - 1),$$

$$\bar{\psi}_4 = 4\eta(1 - \xi - \eta),$$

$$\bar{\psi}_5 = 4\xi(1 - \xi - \eta),$$

and

$$\bar{\psi}_6 = 4\xi\eta.$$

This is the usual piecewise quadratic basis. For the interior element K_j, at least two vertices of which are in the interior of Ω, B_i^j (i=4, 5, 6) is taken at the midpoint of each side. For the boundary element K_j, two vertices of which, B_1^j and B_3^j, are on the boundary Γ, B_6^j is taken at an intersecting point of the boundary and a perpendicular bisector of the side $B_1^jB_3^j$. B_4^j and B_5^j are taken at the midpoints of $B_1^jB_2^j$ and $B_2^jB_3^j$ respectively. Four kinds of Q are considered. In the first case,

$$\bar{\psi}_1 = \bar{\psi}_2 = \bar{\psi}_3 = 0,$$

$\bar{\psi}_4 = 1$ in S_4 and $= 0$ otherwise,

$\bar{\psi}_5 = 1$ in S_5 and $= 0$ otherwise,

and

$\bar{\psi}_6 = 1$ in S_6 and $= 0$ otherwise,

where S_4 is a triangle with vertices A_1, A_2 and G,

and S_5 and S_6 are taken similarly.

In the second case,

$$\bar{\phi}_1=\bar{\phi}_2=\bar{\phi}_3=0,$$

and

$$\bar{\phi}_4=\bar{\phi}_5=\bar{\phi}_6=1/3.$$

In the third case,

$$\bar{\phi}_1=-1/5+3/5\ \eta,$$
$$\bar{\phi}_2=\ 2/5-3/5\ \xi\ -3/5\ \eta,$$
$$\bar{\phi}_3=-1/5+3/5\ \xi,$$
$$\bar{\phi}_4=\ 3/5-4/5\ \xi,$$
$$\bar{\phi}_5=\ 3/5-4/5\ \eta,$$

and

$$\bar{\phi}_6=-1/5+4/5\ \xi\ +4/5\ \eta.$$

In the fourth case,

$$\bar{\phi}_i=\hat{\phi}_i \quad \text{for } i=1,\ldots,\ 6.$$

We conclude this section by stating theoretical results in [1].

Theorem 1.

For each example, (7) and (8) have unique solution $\hat{u}\in S(\Omega_h)$ and the order of its convergence to the exact solution u of (4) and (6) is shown in Table 1.

Here $\tilde{u}$ is a continuous extension of u from $H^m(\Omega)$ into $H^m(\Omega\cup\Omega_h)$ and h is a maximum length of all the sides of the triangles.

3. Numerical Experiments and Their Results

In the first place we consider the following domain,

$$\Omega=\{(x, y);\ \sqrt{x^2+y^2}\ <10\}.$$

As the domain is symmetric with respect to the x-axis and the y-axis, it is sufficient to solve the equation only in a quarter part of it. (Inhomogeneous data f and g are assumed symmetric with respect to both the x-axis and the y-axis.) Its subdivisions and Ω_h are illustrated in Fig. 3, where the upper row corresponds to Example 1 and the lower one corresponds to Example 2. We consider two problems, whose solutions are

$$u=\log(300-x^2-2y^2)-c \tag{9}$$

and

$$u=x^6-2y^4-c, \tag{10}$$

where each c is a constant which is determined from (6). In Figs. 4 and 5, the left graphs show the results in H^1-norm and the right ones in L^2

Table 1　Order of convergence

	Ex.1-1, 1-2, 1-3	Ex.2-1, 2-2	Ex.2-3, 2-4
$\|\hat{u}-\tilde{u}\|_{1,\Omega_h}$	h	h^2	h^2
$\|\hat{u}-\tilde{u}\|_{0,\Omega_h}$	h^2	h^2	h^3

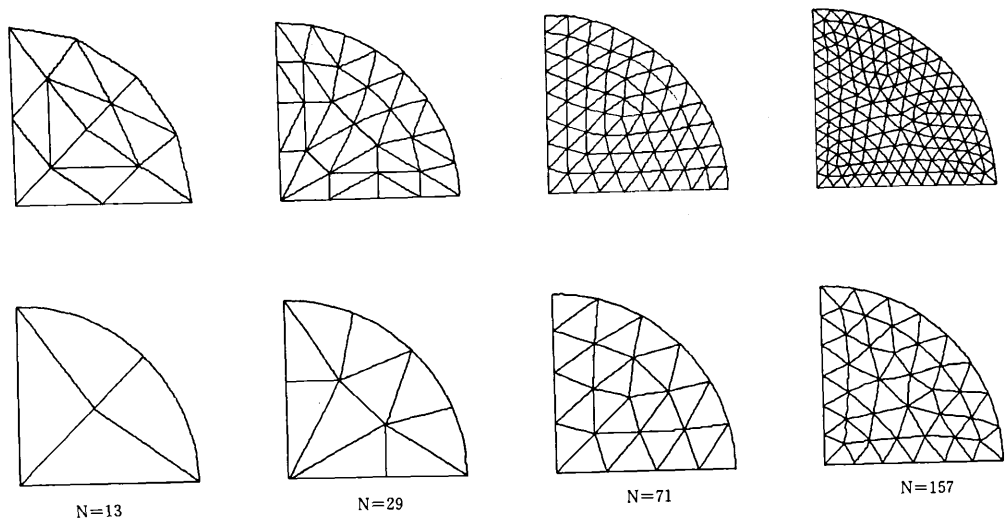

Fig. 3　Subdivisions of the domain

-norm. And $\sqrt{N}$, which is measured by the abscissa, is proportional to h^{-1} since subdivisions may be regarded uniform on the whole. Figs. 4 and 5 are concerned with (9) and (10) respectively. As the results of Examples 1 - 3 and 2 - 4 lie close to the ones of Examples 1 - 1 and 2 - 3 respectively, they are omitted in Figs. 4 and 5.

In the second place we take the following domain,

$$\Omega=\{(x, y); 4<\sqrt{x^2+y^2}<10\}.$$

Its subdivisions and Ω_h are shown in Fig. 6. We take (9) and (10) as the solutions; of course, c takes different value from the former one. Their results are represented in Figs. 7 and 8.

In computing the right hand side of (7), the integral in K_j is converted into one in T_0 by the transformation F_j^{-1} for each j. Tables 2 and 3 give the values of $(\hat{\phi}_i, \bar{\psi}_j)_{T_0}$.

From Theorem 1, the plotted lines in the above graphs should take the following slopes:

-1 in H^1-norm for Examples 1-1 and 1-2,

-2 in H^1-norm for Examples 2-1, 2-2 and 2-3,

-2 in L^2-norm for Examples 1-1, 1-2, 2-1 and 2-2, and

-3 in L^2-norm for Example 2-3.

It can be seen that the slopes of the plotted lines are nearly equel to these values in each graph. The results of Examples 1-1 and 1-2 are not so different from each other. Although the theoretical convergence order of Examples 2-1 is the same as one of Example 2-2, each graph shows that the former gives better approximate solutions than the latter. But it is clear from Table 3 that the former needs more computation than the latter in determining the right hand side of (7).

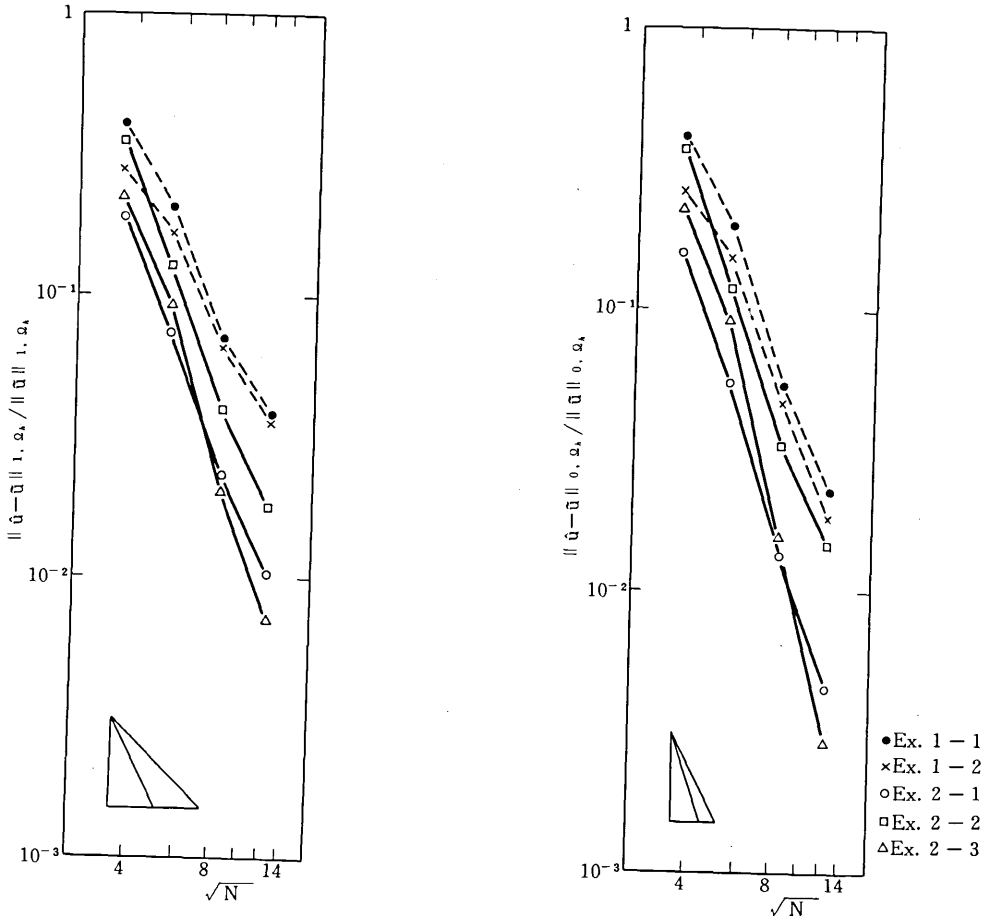

Fig. 4 Relative errors of the approximate solutions

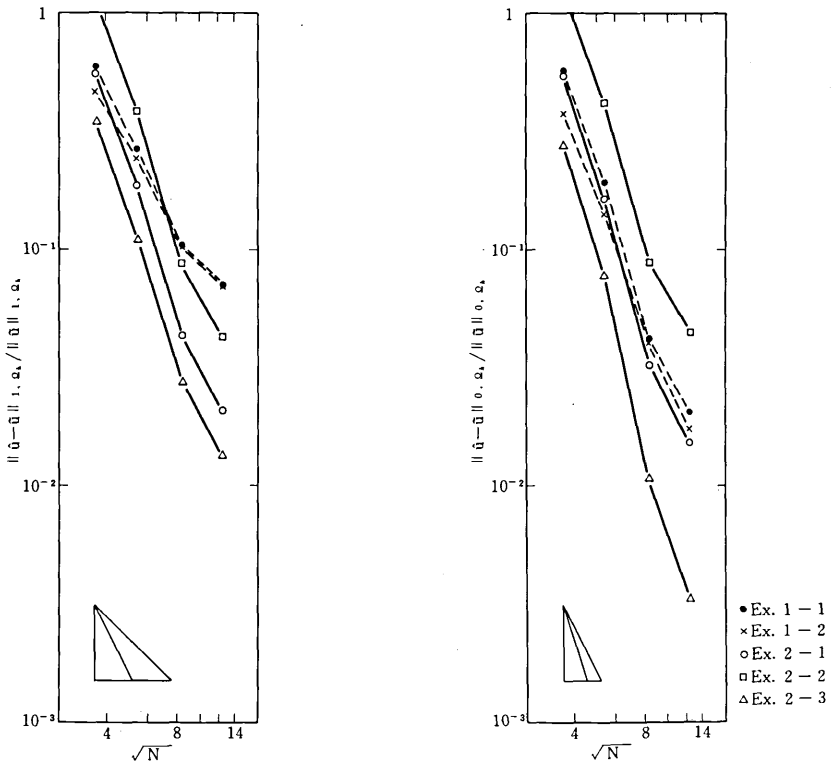

Fig. 5　Relative errors of the approximate solutions

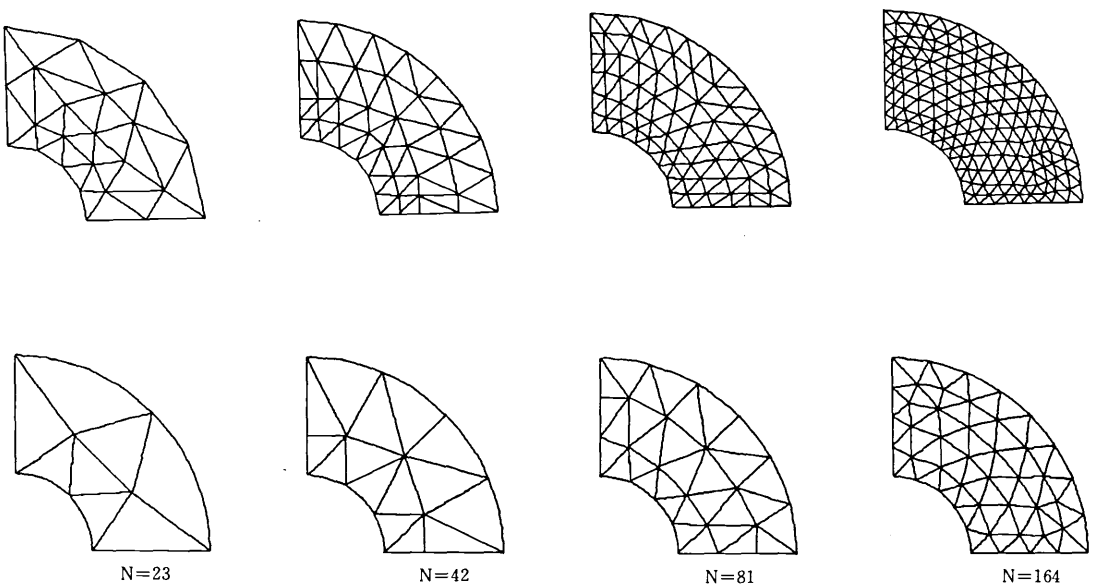

Fig. 6　Subdivisions of the domain

Table 2 Components of $(\phi_i, \bar{\psi}_j)_{\tau_0}$ in Example 1

Ex. 1 — 1

i \ j	1	2	3
1	22	7	7
2		22	7
3	SYM.		7

×1/216

Ex. 1 — 2

i \ j	1	2	3
1	1	1	1
2		1	1
3	SYM.		1

×1/18

Ex. 1 — 3

i \ j	1	2	3
1	2	1	1
2		2	1
3	SYM.		2

×1/24

Table 3 Non-zero components of $(\phi_i, \bar{\psi}_j)_{\tau_0}$ in Example 2

Ex. 2 — 1

i \ j	2	4	6
1	1	−2	1
2	17	5	5
3	1	1	−2
4	5	17	5
5	−2	1	1
6	5	5	17

×1/162

Ex. 2 — 2

i \ j	2	4	6
2	1	1	1
4		1	1
6	SYM.		1

×1/18

Ex. 2 — 3

i \ j	1	2	3	4	5	6
1	6	4	−3	−8	−3	4
2		44	4	28	−8	28
3			6	4	−3	−8
4				44	4	28
5	SYM.				6	4
6						44

×1/600

Ex. 2 — 4

i \ j	1	2	3	4	5	6
1	6	0	−1	−4	−1	0
2		32	0	16	−4	16
3			6	0	−1	−4
4				32	0	16
5	SYM.				6	0
6						32

×1/360

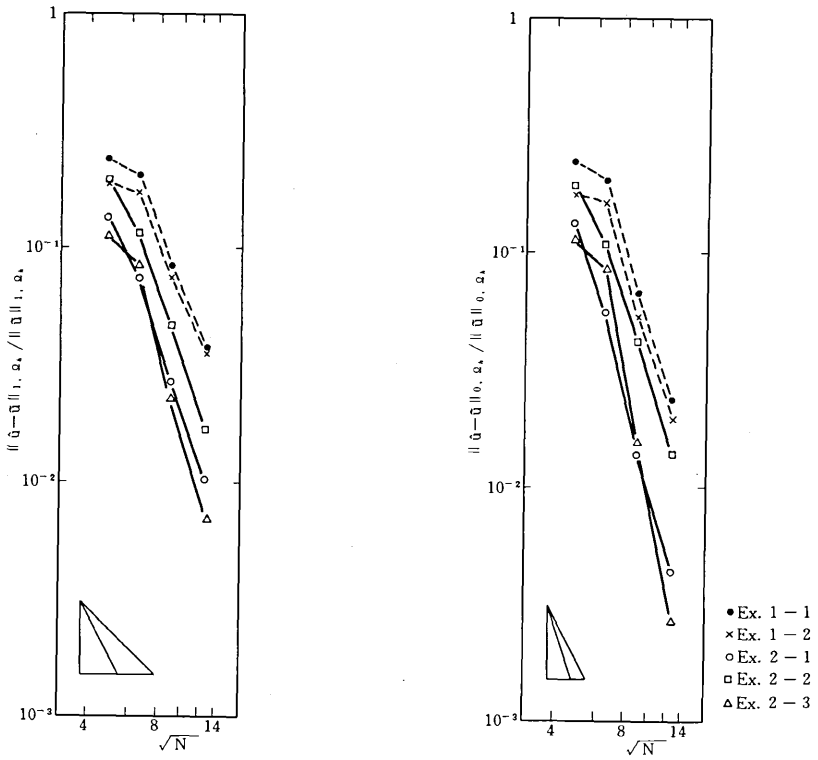

Fig. 7 Relative errors of the approximate solutions

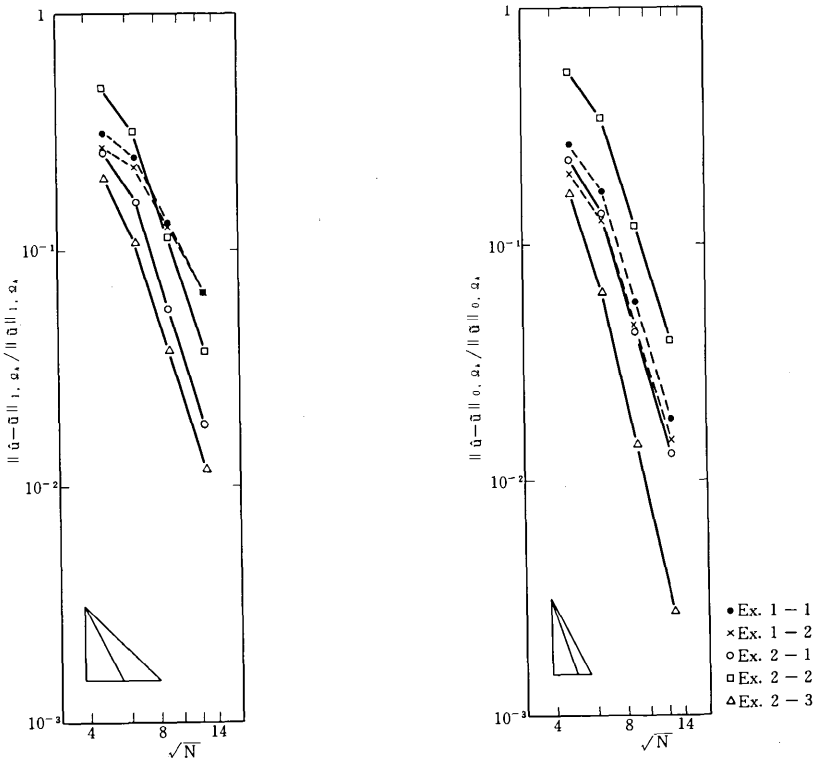

Fig. 8　Relative errors of the approximate solutions

Acknowledgements

The author wishes to express his gratitude to Professor T. Kawai and Professor H. Shibata of University of Tokyo for their encouragement.

(Manuscript received, Oct. 9, 1974)

References

[1] Tabata, M., Higher-order approximate solutions of Neumann problems by the isoparametric finite element method with the relevant lumping operator, to appear in Publ. RIMS. Kyoto Univ.

[2] Friedrichs, K. O. & Keller, H. B., A finite difference scheme for generalized Neumann problems, Numerical solution of partial differential equations, ed. by J. H. Bramble, Academic Press, 1966, 1-19.

[3] Ciarlet, P. G. & Raviart, P. A., Interpolation theory over curved elements, with applications to finite element methods, Computer Methods in Appl. Mech. and Eng. 1, 217-249(1972).